Neurological Disorders & Epilepsy Journal

SCIENTIFIC LITERATURE

Special Issue Article "Guillain-Barré Syndrome" Review Article

Pathology of Early Guillain-Barré Syndrome

José Berciano*

Professor Emeritus of Neurology, University of Cantabria, University Hospital "Marqués de Valdecilla (IDIVAL)" and "Centro de Investigación Biomédica en Red de Enfermedades Neurodegenerativas (CIBERNED)", Santander, Spain

ARTICLE INFO

Received Date: October 28, 2019
Accepted Date: November 30, 2019
Published Date: December 06, 2019

KEYWORDS

Acute inflammatory demyelinating polyneuropathy; Acute motor axonal neuropathy; Axonal degeneration; Demyelination; Endoneurial fluid pressure; Endoneurial inflammatory edema; Experimental autoimmune neuritis; Early Guillain-Barré syndrome; Spinal nerves; Ultrasonography

Citation for this article: José Berciano, Pathology of Early Guillain-Barré Syndrome. Neurological Disorders & Epilepsy Journal. 2019; 2(2):125

Corresponding author:
José Berciano,
Professor Emeritus of Neurology, University of Cantabria, Avda Valdecilla s/n, 39008 Santander, Spain,
Email: joseberciano51@hotmail.com; jaberciano@humv.es

ABSTRACT

Guillain-Barré Syndrome (GBS) is an acute-onset, immune-mediated disorder of the peripheral nervous system, which includes at least four disease patterns: Acute Inflammatory Demyelinating Polyneuropathy (AIDP), acute motor axonal neuropathy, acute motor-sensory axonal neuropathy, and Fisher's syndrome. The aim of this paper was to analyze the pathologic background of early GBS, arbitrarily established up to 10 days of symptom onset. For this purpose, I have carried out a comprehensive literature review of autopsy proven early GBS cases, and an update of our five AIDP patients with autopsy study on whom clinical study was done within 10 days after onset. Pathological changes predominated in proximal nerves, in some studies being more prominent at the sides where the spinal roots unite to form the spinal nerves. Particularly in the first few days of the clinical course, endoneurial inflammatory edema was the outstanding feature. Where appropriate, a comparison of early GBS pathological results with those of experimental autoimmune neuritis is carried out. I provide new insights into the pathogenesis of early GBS.

INTRODUCTION

Guillain-Barré syndrome (GBS) is an acute-onset, immune-mediated disorder of the peripheral nervous system, which is currently divided into several subtypes based on electrodiagnostic, pathological and immunological criteria [1-3]. GBS includes at least four disease patterns: Acute Inflammatory Demyelinating Polyneuropathy (AIDP), Acute Motor Axonal Neuropathy (AMAN), Acute Motor-Sensory Axonal Neuropathy (AMSAN), and Fisher's syndrome. AMAN and AMSAN are disorders frequently associated with serum antibodies against the gangliosides, GM1, GM1b, GD1a or GalNAc-GD1a, and antecedent of infection with Campylobacter jejuni. Fisher's syndrome is associated GQ1b reactivity in the great majority of cases. In Europe and North America, GBS is usually caused by AIDP, whereas in East Asia a considerable number of GBS patients have AMAN or AMSAN [2]; two recent European studies have demonstrated, however, higher prevalence ratios of axonal GBS, which may represent around one third of cases [4,5].

Most GBS patients will have an acute neuropathy reaching a peak within 4 weeks of onset, and this progressive weakness is one of the core diagnostic clinical features of GBS [1]. At the nadir of the disease, the clinical diagnosis of GBS is not difficult for the trained clinical neurologist and relies on diagnostic criteria having stood the test of time [1-3]. This is not the case in early GBS, arbitrarily defined as the 10 days of disease onset, when atypical clinical signs and symptoms may lead to delayed diagnosis [6]. Neurophysiological testing plays a very important role in confirming

diagnosis of peripheral neuropathy and GBS subtype classification, though syndromic subtyping may require serial studies [7-10]. It is a rooted concept that electrical abnormalities in GBS may not be sufficiently widespread for definite diagnosis in the first 2 weeks [11].

Within 30 days after the onset and in cases examined by immune-histochemical studies, the classic GBS pathological hallmark is widespread nerve inflammatory demyelination usually accompanied by a variable degree of secondary axonal degeneration, with greater cell-mediated immunity in some cases and greater antibody targeted macrophage-mediated demyelination and others [12]. This notion is probably not entirely applicable to early stages of GBS. The main aim of this paper is to revise the pathological background of early GBS. For this purpose and on the basis of a previous review [13], the present work is divided into three parts: i/ I will revise so far GBS reported autopsy studies done within 10 days after symptom onset; ii/ I will add our own series of autopsy proven AIDP cases, clinically evaluated within this period of the clinical course; and iii/ I will present concluding remarks from autopsy studies.

AUTOPSY STUDIES IN EARLY GBS: A LITERATURE REVIEW

Table 1 summarizes 51 autopsy reports performed in early GBS according to chronological order of publication [13,14-21].

In the seminal series of 50 autopsied GBS patients, received in the U.S. Army Institute of Pathology during World War II, 32 of them having died between 2 and 10 days after symptomatic onset, Haymaker and Kernohan [14] masterfully described the observed topography and evolution of initial lesions as follows: "As a whole, the observed pathological changes were more prominent in the region where motor and sensory roots join to form the spinal nerve. Oedema of the more proximal part of the peripheral nervous system constituted the only significant alteration the first 3 days of illness. By the fourth day, slight swelling and irregularity of myelin sheaths were detected, and by the fifth, clear-cut disintegration of myelin and swelling of axis cylinders. On the ninth day a few lymphocytes sometimes began to appear, on the eleventh, phagocytes, and on the thirteenth, a proliferation of Schwann cells…The most severe changes were noted in the cases of longest duration, namely 46 days… In all the cases in which appropriate material was available, the degenerative changes, decidedly focal in early stages of the disorder, were concentrated in the region of the spinal nerves and extended both proximally and distally for a short distance, but whether or not peripheral nerves also bore the brunt of the attack could not be determined because of the paucity of peripheral nerve material. Where motor symptoms were most prominent the lesions tended to predominate in the anterior roots, and where widespread anaesthesia accompanied the paralysis the lesions were found in anterior and posterior roots". Given that lymphocytes tended to increase in number as time went on, they were originally regarded as part of a reparative process; in fact, the disorder was characterized by a "polyradiculoneuropathy", in which changes in the amount of protein and in the number of cells in the CSF were regarded as incidental to the disorder. Central chromatolysis was observed in spinal motor neurons and dorsal ganglion neurons (see below), a feature that would be widely confirmed in further works; worthy of note is the observed presence of inflammatory cells in spinal and sympathetic ganglia. As a whole, the authors timely indicated that "on microscopic examinations the brains showed little of significance".

In his GBS autopsy material (3 infantile cases and 4 adult cases), Krücke [22] performed a systematic study of the central and peripheral nervous system, including proximal and distal nerve trunks and sympathetic system (Figure 1A); note that these cases are not included in table 1 given that Krücke carried out a non-individualized description. In this material, endoneurial infiltrates occurred as of 24 hours and were prominent as of the third day. Endoneurial oedema was accompanied by cellular infiltrates; given that there were no isolated serous exudates, as previously reported [14], the author interpreted that edema was an integral part of the inflammatory process. Parenchymal destruction, namely demyelination, was most prominent as of day 14. Initially, lesions were focal predominating in proximal nerve trunks, particularly in spinal nerves where edema was severe enough to cause their swelling visible to the naked eye (Figure 1B,C). In short, this is another masterful paper corroborating the pathogenic role of nerve inflammatory edema and lesional predominance over spinal nerves in early GBS. No lesions were observed in the central nervous system.

Table 1: Autopsy studies in GBS performed up to 10 days after onset [13].

Author and reference	No. of cases	Days after onset	Categorization /electrophysiology	Summary of pathology
Haymaker and Kernohan [14]	32	2-10	GBS / ND	Inflammatory edema followed by demyelination, which predominated in spinal nerves
Asbury et al., [15]	5 (case 1)	1	IP / ND	Fulminant GB showing extensive inflammatory lesions in a perivenular distribution and myelin breakdown, which involved peripheral nerves with preservation of spinal roots
Idem	5 (case 2)	3	IP / ND	Clinically, motor GBS. Intense inflammatory lesions of ventral roots with minimal changes in peripheral nerves. Axonal severance presumably caused by inflammation
Idem	5 (case 3)	4	IP / ND	Clinically, motor GBS. Inflammatory lesions and fiber breakdown, which mainly involved the fourth cranial nerve and ventral roots. Minimal changes in peripheral nerve trunks
Idem	5 (case 4)	6	IP / ND	Widespread though spotty inflammatory demyelination
Idem	5 (case 5)	8	IP / ND	Inflammatory demyelination with axonal degeneration in roots
Kanda et al., [16] and Yokota et al., [17]	1	6	GBS /↓CMAP	Motor GBS showing inflammatory demyelination of spinal roots and spinal nerves, and minimal changes in more distal nerve trunks
Honavar et al., [13]	1 (case 1)	10	GBS / ↓CMAP with absent sural nerve SNAP	Widespread inflammatory demyelination
Ropper and Adelman [18]	1	3	GBS / ND	Mild lymphocytic and macrophage infiltrates in 3 of the 17 peripheral nerve samples and in most lumbar roots, and incipient demyelination
Griffin et al., [19]	2	5,7	AMAN / ↓CMAP	Extensive early wallerian-like degeneration of ventral roots and motor fibers
Idem	3	3-9	AIDP / demyelinating	Severe inflammatory demyelination in motor and sensory fibers
Idem	3	4-9	Minimal pathology/ND	Minimal wallerian-like degeneration of motor and sensory fibers
Griffin et al., [19,20]	2	7,7	AMSAN / ↓CMAP	Early wallerian-like degeneration of motor and sensory fibers more marked in spinal roots
Gallardo et al., [21]	1	9	GBS / ↓CMAP, mild ↑DML, A waves and absence of F waves	Inflammatory edema and mild demyelination of ventral rami of cervical and lumbar nerves, and to a lesser degree of spinal roots and peripheral nerve trunks

Abbreviations: AIDP: Acute Inflammatory Demyelinating Polyneuropathy; AMAN: Acute Motor Axonal Neuropathy; AMSAN: Acute Motor Sensory Axonal Neuropathy; CMAP: Compound Muscle Action Potential; DML: Distal Motor Latency; GBS: Guillain-Barré Syndrome; IP: Idiopathic Polyneuritis; ND: Not Done; SNAP: Sensory Nerve Action Potential

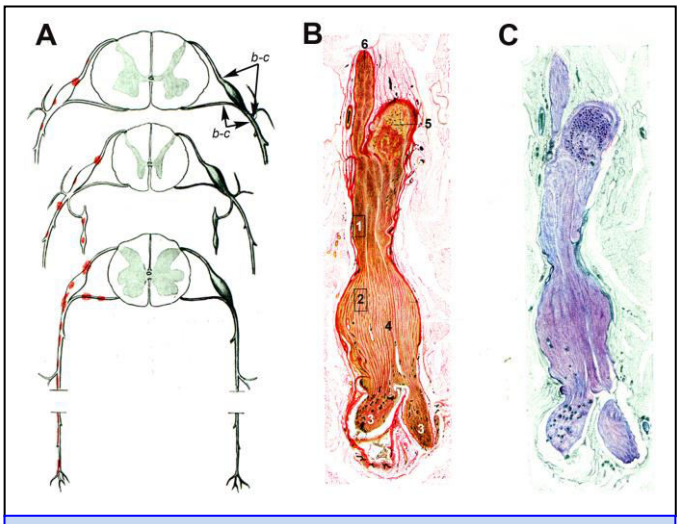

Figure 1: Reproduction of figures 65 to 67 by Krücke [22] with minimal modifications.

(A) Diagram of GBS lesions at cervical (upper row), thoracic (middle row) and sacral (lower row) levels; note that they mainly rely on proximal nerves including ventral and dorsal spinal roots, spinal root ganglia, sympathetic ganglia and ventral rami of spinal nerves (red dots). Lettering b-c indicates nerve segment illustrated in the following two figures. (B) Longitudinal section of the nerve segment between ventral spinal root and spinal nerve from a GBS patient died on day 18, original numbering being as follows: (1 and 2) areas illustrated by the author in other figures (specially his figure 68b showing abundant endoneurial inflammatory edema, which was designated as "mucoid exudate"); (3) rami of the spinal nerve (undoubtedly, ventral and dorsal rami); (4) spindle-shaped swelling of the spinal nerve; (5) spinal root ganglion; and (6) ventral spinal root (Van Gieson, magnification not specified). (C) The same longitudinal section showing a purplish discoloration of the spindle-shaped swelling of the spinal nerve (Cresyl violet, magnification not specified).

Asbury and colleagues reported another comprehensive clinico-pathological series of 19 GBS patients, cases 1-5 being autopsied within 9 days after onset [15]. The authors established that the pathologic hallmark of the disease is a spotty perivenular mononuclear inflammatory infiltrate with segmental demyelination being the predominant form of nerve fiber damage. According to the authors, all levels of the peripheral nervous system are vulnerable to attack, including the anterior and posterior roots, ganglia, proximal and distal nerve trunks and terminal twigs, cranial nerves, and sympathetic chains and ganglia. In contrast to what described Haymaker and Kernohan [14] (see previous paragraph), no pre-inflammatory or edema stage was recognized either in the gross or microscopic state. They stated that some of the emphasis on root pathology doubtlessly reflects the fact that roots have been taken at the autopsy table far more frequently than have peripheral nerves; no level or site in the peripheral nerve is indemnified. Although this notion is probably true in the long run of the clinical course [2,13], it is worth noting that in 2 cases (Nos. 2 and 3) presenting with motor clinical manifestations, lesions predominated in anterior roots, peripheral nerves being minimally involved (Table 1). Moreover, case 2 showed prominent axonal retraction bulbs on silver stains in lumbar roots, which pertinently the authors related with intense inflammatory changes. This patient, that had had an influenza-like illness 10 days prior to admission, probably represents the first description of AMAN. Finally, Asbury and colleagues underlined the similarities between Experimental Autoimmune Neuritis (EAN) and GBS, which are helpful in understanding the events surrounding the onset of GBS and interpreting its pathology. EAN as an experimental model has been criticized for its failure to translate to successful identification of the antigenic targets of autoreactive T cells in GBS; in spite of this, EAN has provided valuable information regarding immune mechanisms contributing to inflammatory neuropathies [23].

Kanda and colleagues reported a fulminant and pure motor GBS patient, aged 47 years, who died 6 days after onset [16] (see Table 1). On day 3, Motor Conduction Velocity (MCV) of median, ulnar and peroneal nerves were preserved, Compound Muscle Action Potential (CMAP) amplitudes being reduced. Sensory Conduction Velocities (SCV) were normal in the median and sural nerves. Myelin-destructive lesions were widespread. Sensory roots were as severely involved as motor roots, and the paraganglionic, extradural portions of the posterior nerve roots, namely spinal nerves [24], were considered to be the site of maximal attack, a fact confirming that spinal nerves are a pathological hot spot in GBS [14,22]. Contrariwise, median (at wrist), sciatic (at hip and knee) and sural nerves (at midcalf and ankle) showed minimal or no lesions. In this case, Yokota and colleagues reported median nerve pathology at the C7 spinal root, elbow and wrist; although typical demyelinating changes predominated in the root, most myelinated fibers were well preserved at the wrist [17].

In 1991, McKhann and colleagues reported clinical and electrophysiological findings in 37 children of post-infectious acute paralytic disease coming from Northern China [25].

According to the observed electrophysiological findings, the authors proposed the hypothesis that the disorder is a reversible distal motor nerve terminal or anterior horn cell disease. Two years later and under the rubric of AMAN, the authors reported the results of 10 autopsy studies showing non-inflammatory wallerian-like degeneration of motor fibers in 5, demyelination in 3, and absence of lesions in 2 [26]. The observed lesions were described as follows: "The most proximal site of fiber degeneration was in the proximal or mid-ventral roots; the proportion of degenerating fibers increased distally toward the ventral root exit from the dura. At this level, up to 80% of motor fibers were degenerating", that is, again maximal pathology occurred in spinal nerves [24].

Afterwards, these histopathological features were reassessed in other seminal studies by the Johns Hopkins' Group and Chinese collaborators [19,20,27,28], the series comprising now 12 postmortem studies, the lesions were categorized as follows: 3 AMAN, 3 AMSAN, 3 AIDP, and 3 exhibiting minimal pathology. Autopsies were performed within 10 days after onset in all but 2 patients (see table 1). In the AMAN pattern, predominant wallerian-like pathology was found within 200 µm of the ventral root exit zone, the stage of this pathology being more advanced in the roots than in the peripheral nerves. In the AMSAN pattern, ventral and dorsal roots as well as peripheral nerves showed early ongoing wallerian-like degeneration. A prominent feature of axonal patterns was the early presence of macrophages within the periaxonal space, surrounding or displacing the axon, and surrounded by an intact myelin sheath with presence of IgG and the complement activation product C3d bound to the axolemma. The authors suggested that AMAN is an antibody- and complement-mediated disorder in which relevant epitopes are present on the nodal and internodal axolemma. In all 3 AIDP patients, the roots were more severely involved than the peripheral nerves.

Case 1 in the series by Honavar and colleagues presented with a 7-day history of tetraparesis predominating in proximal muscles, areflexia and distal sensory loss (see Table 1) [12]. MCVs and DMLs were normal, whereas CMAP amplitudes were severely reduced. SNAP in radial nerve was normal and absent in sural nerve. At autopsy, all nerves examined other than the anterior roots showed demyelination. It is worth noting that despite dorsal root ganglia and spinal axons appeared normal in paraffin sections, semithin sections of spinal roots and peripheral nerves showed moderate to severe depletion of myelinated fibers; furthermore, there were varying degrees of vesicular dissolution of myelin in all the sections. Therefore, absence of demyelination in ventral roots, as indicated in their Table 2, should be taken with caution.

Ropper and Adelman reported a patient, aged 61 years, with severe sensorimotor GBS, who died 72 hours after onset [18]. Mild lesions in this study are indicated in Table 1.

OUR OWN CLINICAL-PATHOLOGICAL STUDIES IN EARLY GBS

We will now focus on our five clinicopathological studies in GBS, presented in chronological order of publication, which demonstrate the relevance of lesions in proximal nerves [21,29-32]. All five patients had been evaluated within the first 10 days of onset, though pathological studies were done between 9 and 60 days after onset. Their rather old ages, from 52 to 83 years, is probably accounted for by the fact that we are dealing with fatal cases, age greater than 40 years being one the features associated with poor prognosis [33].

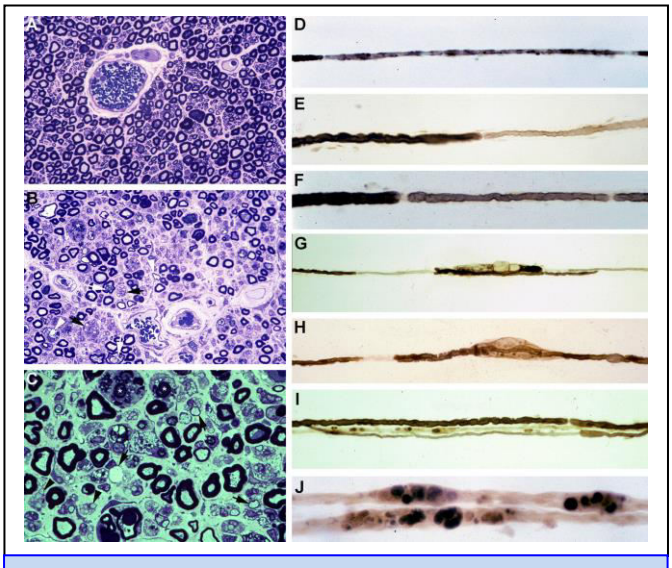

Figure 2: Pathology in pure motor GBS [29].

(A, B) Transverse semithin sections of L5 dorsal (A) and ventral roots (B) period and followed.

Density of myelinated fibers appears preserved in dorsal root and reduced in ventral root (for diameter-frequency histograms, see figure 2 in reference 29). In ventral root note the presence of numerous lipid-laden macrophages, fibers exhibiting vesiculo-vacuolar dissolution of myelin (white arrows), de-remyelinated fibers (white arrowheads), degenerated fibers with myelin collapse indicative of axonal degeneration (asterisks), and clusters of regeneration containing either non-myelinated or re-myelinated axons (black

arrows). No lesions are observed in dorsal root (Toluidine blue; x400 before reduction). (C) Transverse semithin section of L5 ventral root at higher magnification showing numerous endoneurial lipid-laden macrophages sometimes encircling degenerated fibers. Note the presence of de-remyelinated fibers (black arrows), fibers exhibiting axonal degeneration (white asterisks), and clusters of regeneration containing non-myelinated axons (black arrowheads) (Toluidine blue; x630 before reduction). Starting from these semithin sections, it is not an easy task to establish if we are confronted with either a primary demyelinating or an axonal process. (D-J) To clarify the issue we carried out teased fiber preparation from L5 ventral root, which showed the following features: (D) entire internodal demyelination (x100 before reduction); (E, F) entire internodal de-remyelination (x250 before reduction); (G, H) paranodal demyelination and vesiculovacuolar dissolution of myelin (x160 and x100 before reduction); (I) three fibers showing normal texture (upper one), axonal degeneration (middle one), and extensive demyelination (lower one) (x160 before reduction); and (J) wallerian-like degeneration with linear rows of osmiophilic droplets (x400 before reduction).

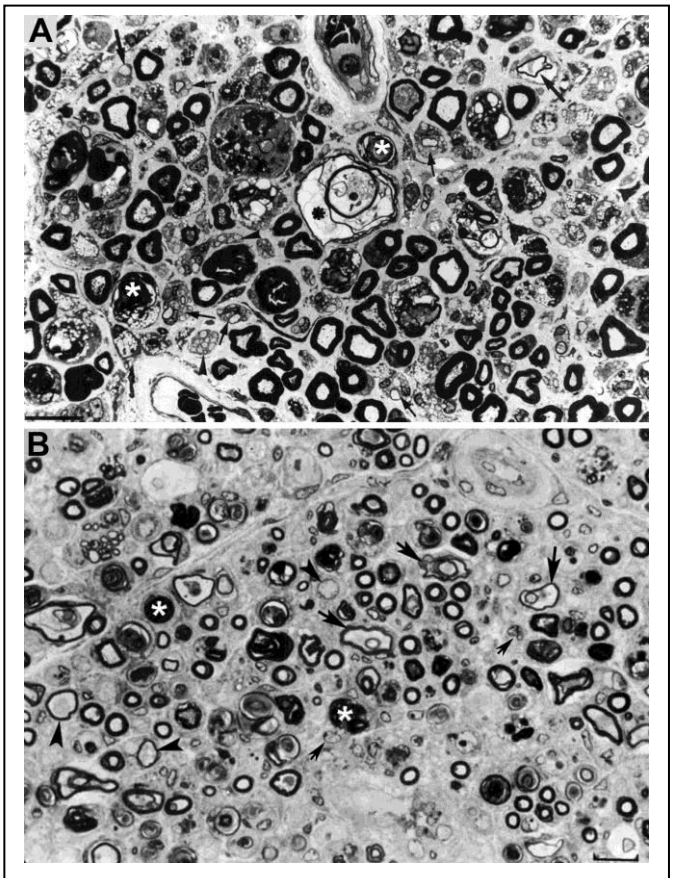

Figure 3: Composite images of figure 3 by Berciano et al [29] (A) and figure 2 by Feasby et al [34] (B).

Both pictures correspond to transverse semithin sections of ventral lumbar roots. (A) Keeping up original graphic resources, note the presence of numerous endoneurial lipid-laden macrophages, sometimes encircling degenerated fibres with myelin collapse (white asterisks). There are clusters of regeneration containing either non-myelinated axons (arrowheads) or non-myelinated and thinly myelinated axons (small arrows), and also occasional demyelinated or remyelinated axons (large arrows). Black asterisk indicates a fiber exhibiting vesiculo-vacuolar dissolution of myelin, this lesion being better illustrated in teased fibre preparation (see figure 2G, H). (Toluidine blue; bar = 19 μm). (B) The original figure legend, with no graphic resources, is as follows [34]: "Transverse section showing severe axonal degeneration". My interpretation is keeping with this criterion, as there are numerous fibers showing myelin collapse (white asterisks), which is indicative of acute axonal degeneration [36]. But note also the presence of fibers with inappropriately thin myelin sheaths (arrowheads) and frequent fibers exhibiting vesiculo-vacuolar dissolution of myelin (large arrows), both features suggesting primary demyelination. In my view, there are frequent endoneurial ovoid or reniform nuclei (small arrows), which most probably correspond to macrophages [36]. (Toluidine blue; bar = 20 μm). (Reproduced with permission from Brain, Oxford University Press).

The first clinico-pathological study concerns a patient, aged 52 years, who presented with a 2-day history of progressive weakness leading to quadriplegia; neither sensory symptoms nor hypoesthesia occurred [29]. Electrophysiology showed normal MCVs with attenuated CMAPs. A working diagnosis of motor-axonal GBS was established [34]. Autopsy, on day 29, showed that the major burden of pathological changes fell on ventral spinal roots consisting of demyelination and secondary axonal demyelination (figure 2). In spinal cord there was extensive central chromatolysis of motor neurons as illustrated below. Lumbosacral plexus showed variable demyelination and wallerian-like degeneration. The observed selective ventral root damage correlates with the well-known magnetic MRI feature of ventral root contrast enhancement in early stages of motor GBS [35]. Our findings corroborate that pure motor GBS may be caused by selective demyelination of ventral spinal roots [16,17]. In 1993 we argued [29] and I continued arguing that ventral lumbar root lesions in our material were similar to those reported by Feasby et al [34], this issue having been taken up again in (Figure 3) [36,37].

The second clinico-pathological report concerns a 67-year-old patient presenting with fulminant AIDP, who died 18 days after onset [30]. Antibodies to C. jejuni were present but there was no antiganglioside reactivity; it is worth noting that an association between C. jejuni infection, characteristic of AMAN, may also occur in AIDP [38]. Three serial electrophysiological studies on days 3, 10 and 17 revealed universal inexcitability of peripheral nerves. Mixed nerve action potentials of median nerve were also absent. We then argued that inexcitability of motor nerves on distal stimulation may be accounted for by

either axonal degeneration or demyelination with conduction block in the terminal segments of the motor axons. Since excitability of motor and sensory nerves in human wallerian degeneration is lost by days 9 and 11 after nerve transection [39], we interpreted that conduction block better explains early nerve inexcitability, though absence of mixed nerve action potentials in median nerve suggests that conduction block involved not only its terminal segment but also the wrist-elbow part. Histological study showed widespread demyelination of spinal roots, and predominantly axonal degeneration of peripheral nerve trunks (Figure 4). This dissociated pattern of pathology between spinal roots and more distal nerve trunks had already been reported in EAN in Lewis rats induced by bovine P2-peptide [40]. In EAN, the severity of lesions correlates with the dose of peptide in the inoculate: low doses result in pure demyelination, whereas axonal degeneration occurs with high doses of antigen. In spite of widespread inflammation, axonal damage in this EAN model was severe in sciatic nerve and almost absent in lumbosacral roots, just as we had observed. In their seminal paper on EAN mediated by T cell line specific for bovine P2-peptide, Izumo and colleagues described that the first signs of clinical disease (flaccid tail and hind-limb weakness) started between 3.5 and 4 days post inoculation (pi) [41]. On day 4 pi, the first evidence of pathologic change appeared, which consisted of marked edema with or without cellular infiltrates in the sciatic nerve and lumbosacral nerve roots, florid demyelination and axonal degeneration not occurring until day 7 pi. Intriguingly, these morphological features mirror electrophysiological investigations showing that, after a latent period of 4 days, rats injected with the higher cell dose showed fulminant paraplegia and complete conduction failure in the sciatic nerve, attributed to severe axonal damage [42]. Potential mechanisms of axonal degeneration in EAN and GBS were discussed by Izumo and colleagues, who wisely wrote "In our animal model of EAN, marked axonal degeneration was observed just 1 to 2 days after intense endoneurial edema… This observation would support the possible role for ischemia in the development of axonal degeneration". We argued that our findings lend support to the hypothesis of increased Endoneurial Fluid Pressure (EFP) in nerve trunks possessing epi-perineurium as the cause of axonal pathology in early stages of the current fulminant form of GBS, and that this called for performing proximal-to-distal analysis of spinal roots and more distal nerve trunks to establish whether or not the appearance of epi- perineurium determines any change in the degree of axonal degeneration [30]. It is timely to remember that spinal roots traverse the subarachnoid space covered by an elastic multicellular root sheath derived from the arachnoid and penetrate the subarachnoid angle (Figure 5). External to this angle, nerve roots (spinal nerves) possess epiperineurium and endoneurium as in the peripheral nerve trunks [43].

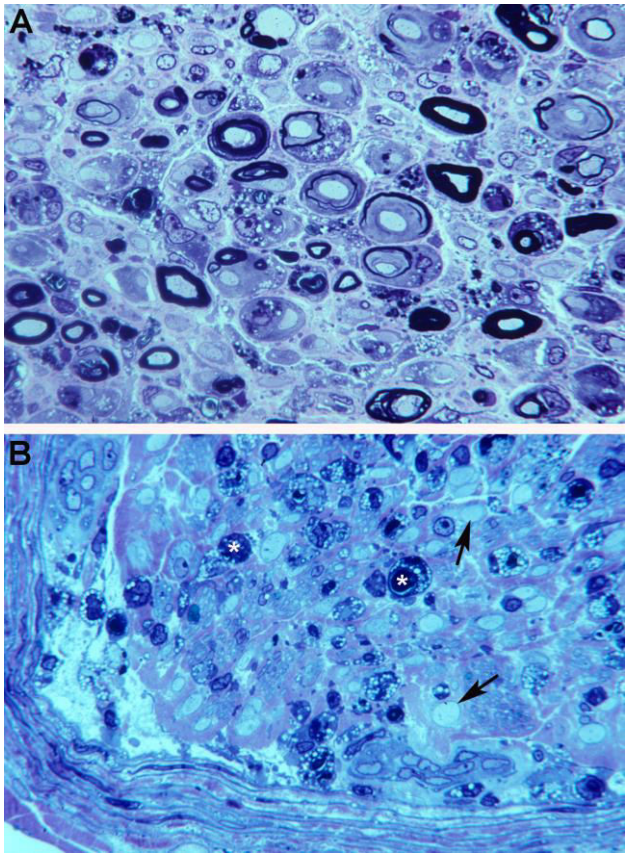

Figure 4: Pathology in fulminant GBS with universal nerve inexcitability [30].

(A) Semithin section of L5 ventral root showing massive demyelination and numerous lipi-laden macrophages (Toluidine blue; x630 before reduction). (B) Semithin section of femoral nerve illustrating marked axonal degeneration (asterisks). Note the presence of denuded axons (arrows) and endoneurial and subperineurial macrophage infiltrates (Toluidine blue, x630 before reduction).

In the third clinico-pathological report, we aimed at establishing if axonal damage in severe AIDP correlates with the appearance of epiperineurium in nerve trunks [31]. A patient, aged 79 years, presented with a 2-day history of distal paresthesias and ascending weakness culminating in

quadriplegia and mechanical ventilation; he died 60 days after onset. Neither antiganglioside nor C. jejuni antibodies were detected. Serial electrophysiological studies (days 4, 17, and 50) initially showed normal nerve conduction velocities with further slowing to the demyelinating range, progressive attenuation of CMAPs, absent SNAPs, and profuse muscle denervation. Pathological study included preforaminal anterior and posterior L3 and L5 spinal roots, third and fifth spinal nerves and their branches, and femoral and sural nerves. Mild de-remyelination was observed in lumbar roots. Axonal degeneration was the predominant lesion in sural nerve. In both lumbar nerves and their branches, there were extensive de-remyelination and centrofascicular or wedge-shape areas with marked loss of large myelinated fibres (Figure 6), a feature which had already been reported in EAN [40]. Such focal endoneurial lesions are characteristic of nerve ischemia involving watershed zones of poor perfusion [44]. In EAN, axonal damage in sciatic nerve is preceded by a significant increase of the endoneurial extracellular space, which is correlated with an increase of EFP causing constriction of transperineurial vessels with pathogenic diminution of nerve blood flow [45]. We argued that the absence of epi-perineurium in spinal roots probably prevents their having an increase of EFP and ischemic injury in spite of inflammatory demyelination. Perineurium is relatively inelastic and has only a limited ability to expand. Small increases of EFP, as caused by endoneurial inflammation [41,44,45], can be accommodated, but any increase beyond these limits, as presumably occurs in early stages of severe or fulminant forms of GBS, will produce an increase in EFP, leading to distal axonal degeneration (Figure 5). Parallel to the distribution of endoneurial inflammatory changes, nerve ischemia could account for early partial or complete conduction block or even for universal inexcitability [30,46]. Despite accumulation of ischemic areas distally, it is conceivable that just partial preservation of one or several nerve fascicles could explain attenuated CMAP with normal MCV, as occurred at first electrophysiological evaluation of the current patient. Quick clinical recovery, occasionally reported in other GBS cases, could be related to the fact that conduction is rapidly re-established with restoration of nerve flow [44]. Obviously, our pathogenetic proposal does not exclude the contribution of primary myelin or axonal pathology to early electrophysiological abnormalities. Later electrophysiologic features will rely on such myelin, axonal, or both pathologies.

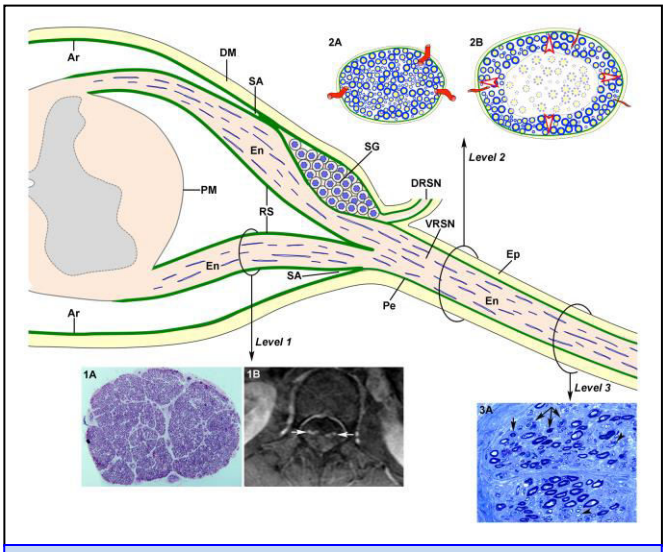

Figure 5: Diagram of spinal root and spinal nerve microscopic anatomy [13].

As of Subaracnoid Angle (SA), the Epineurium (Ep) is in continuity with the Dura Mater (DM). The Endoneurium (En) persists from the peripheral nerves through the spinal roots to their junction with the spinal cord. At the SA, the greater portion of the Perineurium (Pe) passes between the dura and the Arachnoid (Ar), but a few layers appear to continue over the roots as the inner layer of the Root Sheath (RS). The arachnoid is reflected over the roots at the SA and becomes continuous with the external layers of the RS. At the junction with the spinal cord, the outer layers become continuous with the pia mater (PM). Immediately beyond the Spinal Ganglion (SG), at the SA, the ventral and dorsal nerve roots unite to form the spinal nerve, which emerges through the intervertebral foramen and divides into a dorsal ramus (DRSN) and a Ventral Ramus (VRSN). Therefore intrathecal nerve roots are covered by an elastic root sheath derived from the arachnoid, whereas spinal nerves possess epi-perineurium which is relatively inelastic. Proximal-to-distal early GBS inflammatory lesions are illustrated as follows: ventral lumbar root (level 1), spinal nerve (level 2) and sciatic nerve (level 3). At level 1, this semithin complete cross section of ventral L5 root shows preservation of the density myelinated fibers (1A), though inflammatory lesions, observable at higher augmentation (not shown), may account for increased surface area, and thickening and contrast enhancement of ventral roots on spinal MRI (1B, arrows). Both cartoons at level 2 illustrate the following features: i/ normal anatomy of spinal nerve, usually monofascicular with epi-perineurial covering (2A), which account for its sonographic appearance usually consisting of a hypoechoic oval structure surrounded by hyperechoic perineurial rim; and ii/ endoneurial inflammatory edema may cause a critical elevation in EFP that constricts transperineurial vessels by stretching the perineurium beyond the compliance limits (2B, arrowheads), which could result in areas of endoneurial ischemia, here centrofascicular. As illustrated here (2A vs 2B), despite low spinal nerve compliance, early inflammatory events in GBS may cause an

increase of CSA; moreover, perineurial inflammation (see figure 8) accounts for loss of hyperechoic perineurial rim (see figure 7). At level 3, this cross semithin section of sciatic nerve from a fatal AIDP patient shows several myelinated fibers exhibiting wallerian-like degeneration (myelin collapse, arrows) secondary to more proximal demyelinating lesions; note the presence of remyelinated fibers (arrowheads) and lipid-laden macrophages. Without knowledge of proximal nerve pathology, such distal florid wallerian-like lesions would make it very difficult to reach an accurate diagnosis. Diagram inspired by figure 3-6 from Berthold and colleagues [43].

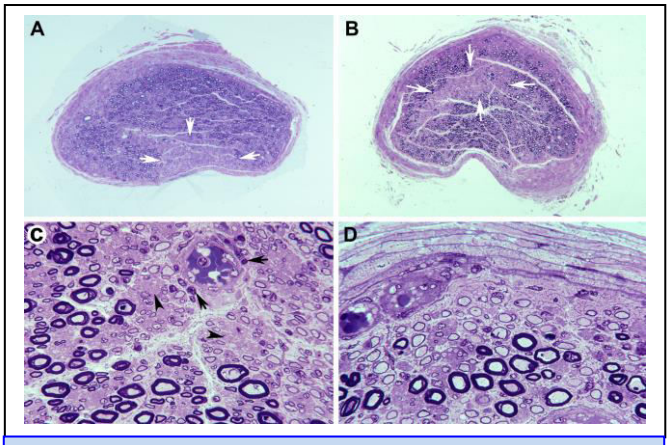

Figure 6: Proximal nerve ischemic lesions in AIDP [31].

(A) Semithin cross-section of the third lumbar nerve showing a wedge-shape area (arrows) with marked loss of myelinated fibers (Toluidine blue; x62 before reduction). (B) Semithin cross-section of the lumbosacral trunk with a centrofascicular area (arrows) also exhibiting marked loss of myelinated fibers (Toluidine blue; x62 before reduction). Both in A and B note apparent widespread diminution of myelinated fibers. (C) This high-power view of the central region of the lumbosacral trunk illustrates severe reduction of large myelinated fibers, thinly myelinated small axons, preserved unmyelinated axons (arrowheads), and widespread endoneurial mononuclear inflammatory cells, some of them with perivascular distribution (arrows) (Toluidine blue; x375 before reduction). (D) This high-power view of the subperineurial region of the lumbosacral trunk shows numerous de-remyelinated fibers and mononuclear cells; such extensive demyelination accounts, to some degree, for the apparent widespread loss of myelinated fibers observed in A and B (Toluidine blue; x475 before reduction).

In the fourth clinicopathological report we described a severe GBS patient, aged 83 years, in whom two serial electrophysiological studies (days 3 and 10) showed an axonal pattern [32]. Neither antiganglioside nor C. jejuni antibodies were detected. Autopsy on day 30 showed that the brunt of pathology, combining extensive and primary de-remyelination with secondary axonal degeneration and areas of ischemia, relied on spinal nerves, such pathology implying axonal degeneration in more distal nerve trunks. Corroborating Haymaker and Kernohan's findings [14] (see above), there was central chromatolysis involving spinal motor neurons and root ganglion cells (Figure 7). As in a previous study [32], we observed the presence of dark fibers (Figure 8), bringing to mind dark swollen axons. Our thin sections revealed, however, that dark areas corresponded not to swollen axons but to ridges of adaxonal Schwann cells replete with degenerated organelles, axons being preserved or at most with a reduced caliber. Such Schwann cell/axon interactions likely represent a nonspecific mechanism by which the Schwann cell clears debris and helps maintain the integrity of the axon. In this way, both central chromatolysis and dark fibers represent reparative phenomena. Lastly, this case exemplifies that without detailed pathologic examination, a precise diagnosis of AIDP would have never been reached.

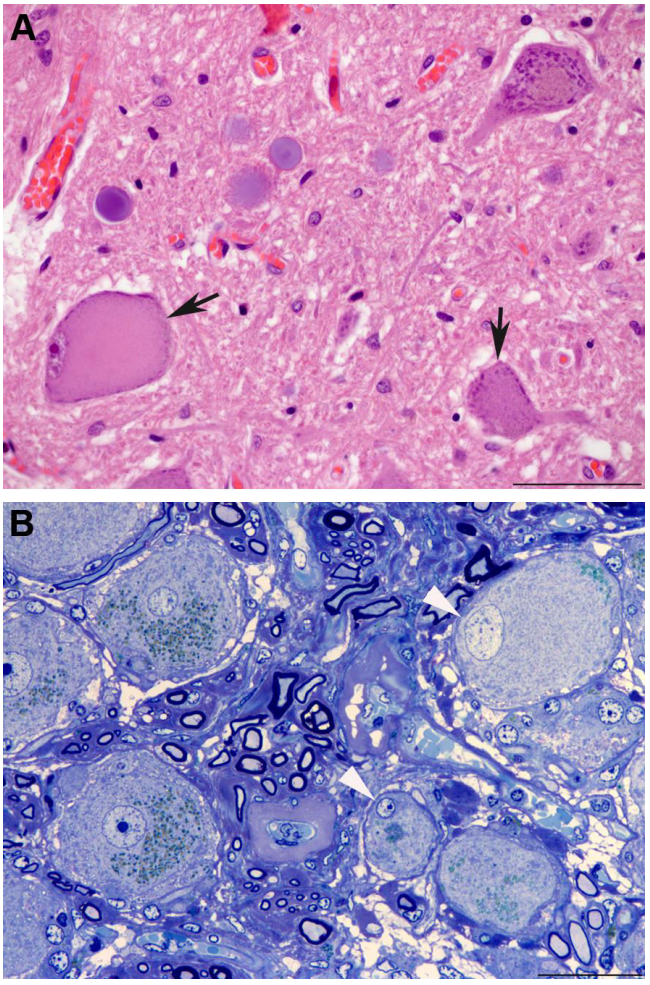

Figure 7: Central chromatolysis in spinal neurons from a severe AIDP patient with secondary axonal degeneration [32].

(A) Chromatolysis in two of the three illustrated lumbar anterior horn cells (arrows) (Paraffin, H&E, bar = 90 μm). (B) Semithin

section of posterior L5 ganglion showing several normal neurons and two exhibiting central chromatolysis with eccentric nuclei (arrowheads) (Toluidine blue, bar = 65 μm). Central chromatolysis and dark fibers (see next figure) represent reparative changes to axonal damage (for further discussion, see reference 32).

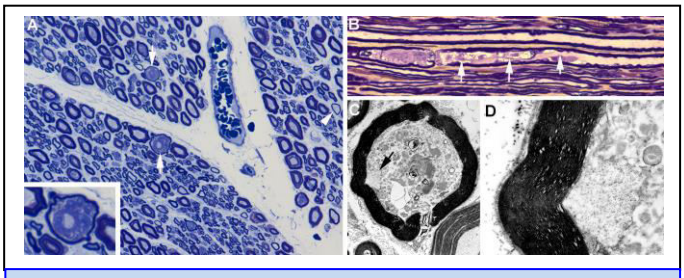

Figure 8: Dark fibers in severe AIDP: another reparative change of axonal dysfunction [32].

(A) Cross semithin section of L5 dorsal root showing normal appearance of most fibers and the presence of occasional remyelinated fibers (arrowhead), and dark fibers (arrows); inset shows one of the dark fibers at higher magnification consisting of normal myelin sheath and dark content with a light core. Dark fiber texture is better shown in longitudinal sections. (B) Semithin longitudinal section of L5 dorsal root showing a large myelinated fiber with extensive material accumulation in the adaxonal Schwann cell cytoplasm, which is more pronounced in the paranodal region; note that the axon is variably displaced but otherwise preserved (arrows). (C) This electron micrograph section of L5 dorsal root shows the morphology of a dark fiber characterized by a compressed and eccentrically located axon (arrow) surrounded by complex adaxonal Schwann cell processes containing vacuoles, degenerated organelles, and amorphous material. (C) At higher magnification, note preservation of the axonal neurofilaments. Bars: (A) 24 μm; (B) 20 μm; (C) 3.2 μm; (D) 0.9 μm.

The fifth clinicopathological study was done in a patient included, as case 1, in our nerve US study [21]. She was an 80-year-old patient admitted with a 4–day history of foot paresthesias and ascending weakness leading to flaccid quadriplegia and areflexia requiring mechanical ventilation on day 5. The patient was treated with standard Intravenous Immunoglobulin (IVIg) cycles (2gr/kg/day in five days) followed by three boluses 500 mgs/day of intravenous methylprednisolone. Electrophysiological findings on day 5 are summarized in (Table 1). The results of nerve US studies are illustrated in (Figure 9); in short, main sonographic changes relied on the ventral rami of C5-C7 nerves and consisted of enlargement of their cross sectional areas with blurred boundaries. Severe cardiac dysautonomia led to death 9 days after onset. There was nerve inflammatory edema and mild demyelination predominating in ventral rami of spinal nerves (Figure 10).

The mechanism of proximal lesion predominance in early GBS deserves a brief comment. Experimentally, blood-nerve interface is less efficient in several important structures in the peripheral nervous system, including from the spinal cord to the root-nerve junction (spinal nerve), dorsal root ganglia and neuromuscular junctions [47,48]; hence these sites are believed to be especially vulnerable to inflammatory neuropathies. In addition, the pathogenic relevance of proximal nerve trunk lesions in early AIDP and early AMAN has been demonstrated by means of lumbar root stimulation [49] and triple stimulation technique [50], respectively.

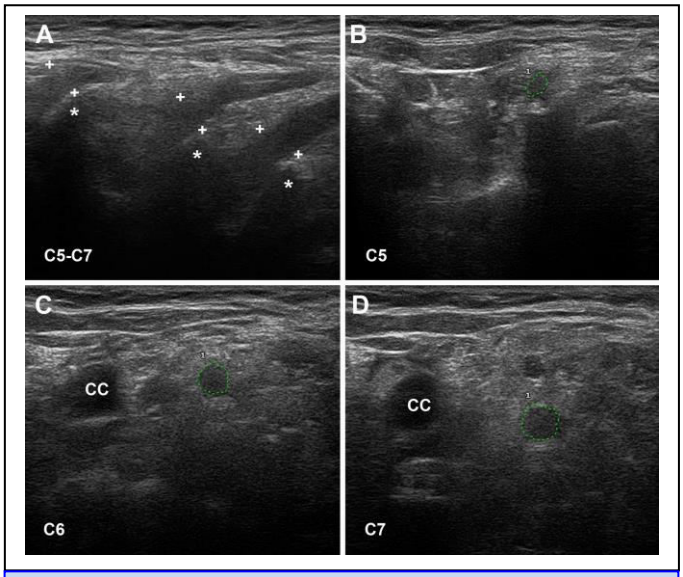

Figure 9: Cervical nerve ultrasonography in AIDP [21].

For pathological data of ventral ramus of C6 nerve see figure 1 in reference 21. (A) Sagittal sonogram showing blurred boundaries of the 3 scanned cervical nerves (callipers). Asterisks indicate transverse vertebral processes. (B-D) Short-axis sonograms showing increased cross sectional areas of ventral rami of C6-C7 nerves (dotted green tracings; for values see reference 21); note that perineurial hyperechoic rims are not identified and that the edge between the nerve and the surrounding fat is not clear. CC indicates common carotid artery.

AUTOPSY STUDIES IN EARLY GBS: CONCLUDING REMARKS

Pathological features of early GBS could be summarized as follows: i/ predominant lesions are usually localized in proximal nerves, a notion applicable to both AIDP and AMAN; ii/ lesional patterns may aggravate and change in the transition from spinal roots to spinal nerves; iii/ as in EAN, early endoneurial inflammatory edema may induce an increase of EFP causing ischemic damage and conduction failure in nerve trunks possessing epi- perineurium, namely from spinal nerves

to pre-terminal nerve branches; iv/ besides AMAN, the pathologic hallmark of pure motor GBS may be selective demyelination of ventral spinal roots; and v/ even after serial nerve conduction studies, electrophysiologically axonal GBS may result from a proximal demyelinating process with secondary axonal degeneration.

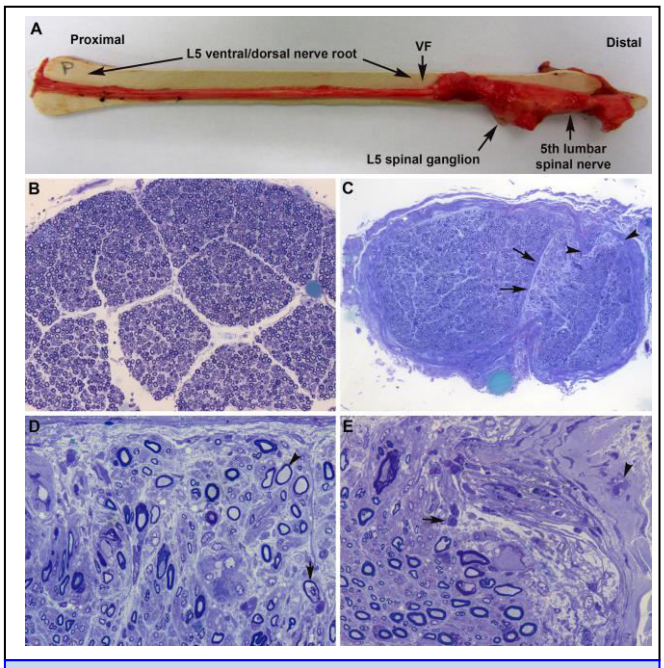

Figure 10: Pathological features in early AIDP [21].

(A) After being dissected down, macroscopic appearance of the right L5 spinal root, L5 spinal ganglion and fifth lumbar spinal nerve. Whereas the preforaminal root shows normal morphology, as of the vertebral foramen (VF) note visible nerve enlargement. (B) Semithin cross-section of L5 ventral root, taken 1 cm above its entrance to the VF, showing that the density of myelinated fibers is preserved (Toluidine blue; original magnification x100 before reduction). (C) Semithin cross-section of the ventral ramus of the fifth lumbar nerve, taken at its emergence trough intervertebral foramen, showing widespread endoneural edema, which is more conspicuous in some subperineurial areas (arrows and arrowheads); such edema results in a spacing out phenomenon giving an observer the false impression of reduced density of myelinated fibers (Toluidine blue; original magnification x65 before reduction). (C) High-power view of the subperineurial area arrowed in B. Note the presence of inflammatory edema with numerous mononuclear cells, fibers with inappropriately thin myelin sheaths (arrowhead), and fibers exhibiting myelin vacuolation (arrow) (Toluidine blue; original magnification x630 before reduction). (D) High-power view of the perineurial and subperineurial area indicated with arrowheads in B. Conspicuous edema is accompanied by the presence of endoneurial (arrow) and perineurial (arrowhead) mononuclear cells (Toluidine blue; original magnification x630 before reduction).

ACKNOWLEDGEMENTS

We wish to thank my colleagues at the University Hospital "Marqués de Valdecilla (IDIVAL)" for their clinical support, Drs Antonio García and Pedro Orizaola for electrophysiological studies, Dr Elena Gallardo for sonographic studies, Dr Nuria Terán-Villagrá for allowing me to have autopsy material, Prof. Miguel Lafarga and María T. Berciano for histological studies, and Mrs Marta de la Fuente for secretarial help.

REFERENCES

1. van Doorn PA, Ruts L, Jacobs BC. (2008). Clinical features, pathogenesis, and treatment of Guillain-Barré syndrome. Lancet Neurol. 7: 939-950.
2. Kuwabara S, Yuki N. (2013). Axonal Guillain-Barré syndrome: concepts and controversies. Lancet Neurol. 12: 1180-1188.
3. Wakerley BR, Uncini A, Yuki N, GBS Classification Group, GBS Classification Group. (2014). Guillain-Barré and Miller Fisher syndromes-new diagnostic classification. Nat Rev Neurol. 10: 537-544.
4. Benedetti L, Briani C, Beronio A, Massa F, Giorli E, et al. (2019). Increased incidence of axonal Guillain-Barré syndrome in La Spezia area of Italy: A 13-year follow-up study. J Peripher Nerv Syst. 24: 80-86.
5. Sedano MJ, Orizaola P, Gallardo E, García A, Pelayo-Negro AL, et al. (2019). A unicenter, prospective study of Guillain-Barré syndrome in Spain. Acta Neurol Scand. 139: 546-554.
6. Vucic S, Cairns KD, Black KR, Chong PST, Cros D. (2004). Neurophysiologic findings in early acute inflammatory demyelinating polyradiculoneuropathy. Clin Neurophysiol. 115: 2329-2235.
7. Dubey D, Kapotic M, Freeman M, Sawhney A, Rojas JC, et al. (2016). Factors contributing to delay in diagnosis of Guillain-Barré syndrome and impact on clinical outcome. Muscle Nerve. 53:384-387.
8. Fokke C, van den Berg B, Drenthen J, Walgaard C, van Doorn PA, et al. (2014). Diagnosis of Guillain-Barré syndrome and validation of Brighton criteria. Brain. 137: 33-43.
9. Hadden RD, Cornblath DR, Hughes RA, Zielasek J, Hartung HP, et al. (1998). Electrophysiological classification of Guillain-Barré syndrome: clinical associations and outcome. Ann Neurol. 44: 780-788.

10. Uncini A, Manzoli C, Notturno F, Capasso M. (2010). Pitfalls in electrodiagnosis of Guillain-Barré syndrome subtypes. J Neurol Neurosurg Psychiatry. 81: 1157-1163.
11. Albers JW, Donofrio PD, McGonagle TK. (1981). Sequential electrodiagnostic abnormalities in acute inflammatory demyelinating polyradiculoneuropathy. Muscle Nerve. 8: 528-553.
12. Honavar M, Tharakan JK, Hughes RA, Leibowitz S, Winer JB. (1991). A clinicopathological study of the Guillain-Barré syndrome. Nine cases and literature review. Brain. 114: 1245-1269.
13. Berciano J, Sedano MJ, Pelayo-Negro AL, García A, Orizaola P, et al. (2017). Proximal nerve lesions in early Guillain-Barré syndrome: implications for pathogenesis and disease classification. J Neurol. 264: 221-236.
14. Haymaker WE, Kernohan JW. (1949). The Landry-Guillain-Barré syndrome; a clinicopathologic report of 50 fatal cases and a critique of the literature. Medicine (Baltimore). 28: 59-141.
15. Asbury AK, Arnason BG, Adams RD. (1969). The inflammatory lesion in idiopathic polyneuritis. Its role in pathogenesis. Medicine (Baltimore). 48: 173-215.
16. Kanda T, Hayashi H, Tanabe H, Tsubaki T, Oda M. (1989). A fulminant case of Guillain-Barré syndrome: topographic and fibre size related analysis of demyelinating changes. J Neurol Neurosurg Psychiatry. 52: 857-64.
17. Yokota T, Kanda T, Hirashima F, Hirose K, Tanabe H. (1992). Is acute axonal form of Guillain-Barré syndrome a primary axonopathy? Muscle Nerve. 15: 1211-1213.
18. Ropper AH, Adelman L. (1992). Early Guillain-Barré syndrome without inflammation. Arch Neurol. 49: 979-981.
19. Griffin JW, Li CY, Ho TW, Xue P, Macko C, et al. (1995). Guillain-Barré syndrome in northern China. The spectrum of neuropathological changes in clinically defined cases. Brain. 118: 577-595.
20. Griffin JW, Li CY, Ho TW, Tian M, Gao CY, et al. (1996). Pathology of the motor-sensory axonal Guillain-Barré syndrome. Ann Neurol. 39: 17-28.
21. Gallardo E, Sedano MJ, Orizaola P, Sánchez-Juan P, González-Suárez A, et al. (2015). Spinal nerve involvement in early Guillain-Barré syndrome: A clinico-electrophysiological, ultrasonographic and pathological study. Clin Neurophysiol. 126: 810-819.
22. Krücke W. (1955). Die primär-entzündliche Polyneuritis unbekannter Ursache. In: Lubarsch O, editor. Handbuch der speziallen pathologischen Anatomie und Histologie, Vol XIII/5, Erkrankungen des peripheren und des vegetativen Nerven. Springer-Verlag, Berlin.
23. Soliven B. (2014). Animal models of autoimmune neuropathy. ILAR J. 54: 282-289.
24. Gray H, Davis DV, Coupland RE, (1967). Gray's anatomy. Described and applied (34th Edition). Longmans, London. pp1217-1243.
25. McKhann GM, Cornblath DR, Ho T, Li CY, Bai AY, et al. (1991). Clinical and electrophysiological aspects of acute paralytic disease of children and young adults in northern China. Lancet. 338: 593-597.
26. McKhann GM, Cornblath DR, Griffin JW, Ho TW, Li CY, et al. (1993). Acute motor axonal neuropathy: a frequent cause of acute flaccid paralysis in China. Ann Neurol. 33: 333-342.
27. Griffin JW, Li CY, Macko C, Ho TW, Hsieh ST, et al. (1996). Early nodal changes in the acute motor axonal neuropathy pattern of the Guillain-Barré syndrome. J Neurocytol. 25: 33-51.
28. Hafer-Macko CE, Sheikh KA, Li CY, Ho TW, Cornblath DR, et al. (1996). Immune attack on the Schwann cell surface in acute inflammatory demyelinating polyneuropathy. Ann Neurol. 39: 625-635.
29. Berciano J, Coria F, Montón F, Calleja J, Figols J, et al. (1993). Axonal form of Guillain-Barré syndrome: evidence for macrophage-associated demyelination. Muscle Nerve. 16: 744-751.
30. Berciano J, Figols J, García A, Calle E, Illa I, et al. (1997). Fulminant Guillain-Barré syndrome with universal inexcitability of peripheral nerves: a clinicopathological study. Muscle Nerve. 20: 846-857.
31. Berciano J, García A, Figols J, Muñoz R, Berciano MT, et al. (2000). Perineurium contributes to axonal damage in acute inflammatory demyelinating polyneuropathy. Neurology. 55: 552-559.
32. Berciano J, García A, Villagrá NT, González F, Ramón C, et al. (2009). Severe Guillain-Barré syndrome: sorting out

the pathological hallmark in an electrophysiological axonal case. J Peripher Nerv Syst. 14: 54-63.

33. Sedano MJ, Calleja J, Canga E, Berciano J. (1994). Guillain-Barré syndrome in Cantabria, Spain. An epidemiological and clinical study. Acta Neurol Scand. 89: 287-292.
34. Feasby TE, Gilbert JJ, Brown WF, Bolton CF, Hahn AF, et al. (1986). An acute axonal form of Guillain-Barré polyneuropathy. Brain. 109: 1115-1126.
35. Byun WM, Park WK, Park BH, Ahn SH, Hwang MS, et al. (1998). Guillain-Barré syndrome: MR imaging findings of the spine in eight patients. Radiology. 208: 137-141.
36. King RHM. (1999). Atlas of peripheral nerve pathology. London, Oxford University Press.
37. Berciano J. (2018). Axonal pathology in early stages of Guillain-Barré syndrome. Neurologia. S0213-4853(18)30176-2.
38. Drenthen J, Yuki N, Meulstee J, Maathuis EM, van Doorn PA, et al. (2011). Guillain-Barré syndrome subtypes related to Campylobacter infection. J Neurol Neurosurg Psychiatry. 82: 300-305.
39. Chaudry V, Cornblath DR. (1992). Wallerian degeneration in human nerves: serial electrophysiological studies. Muscle Nerve. 15: 687-692.
40. Hahn AF, Feasby TE, Wilkie Lougren D. (1991). P2-peptide induced experimental allergic neuritis: a model to study axonal degeneration. Acta Neuropathol. 82: 60-65.
41. Izumo S, Linington C, Wekerle H, Meyermann R. (1985). Morphologic study on experimental allergic neuritis mediated by T cell line specific for bovine P2 protein in Lewis rats. Lab Invest. 53: 209-218.
42. Heininger K, Stoll G, Linington C, Toyka KV, Wekerle H. (1986). Conduction failure and nerve conduction slowing in experimental allergic neuritis induced by P2-specific T-cell lines. Ann Neurol. 19: 44-49.
43. Berthold CH, Fraher JP, King RHM, Rydmark M. (2005). Microscopical anatomy of the peripheral nervous system. In: Dyck PJ and Thomas PK. eds., Peripheral neuropathy. Philadelphia, WB Saunders. 1: 35-91.
44. McManis PG, Low PA, Lagerlund TD. (1993). Nerve blood flow and microenviroment. In: Peripheral neuropathy. In: Dyck PJ et al. eds., Peripheral neuropathy. Philadelphia, WB Saunders, vol 1, pp 453-473.
45. Powell HC, Myers RR, Mizisin AP, Olee T, Brotoff SW. (1991). Response of the axon and barrier endothelium to experimental allergic neuritis induced by autoreactive T cell lines. Acta Neuropathol. 82: 364-377.
46. Fuller GN, Jacobs JM, Lewis PD, Lane RJ. (1992). Pseudoaxonal Guillain-Barré syndrome: severe demyelination mimicking axonopathy. A case with pupillary involvement. J Neurol Neurosurg Psychiatry. 55: 1079-1083.
47. Olsson Y. (1968). Topographical differences in the vascular permeability of the peripheral nervous system. Acta Neuropathol. 1968; 10: 26-33.
48. Kanda T. (2013). Biology of the blood-nerve barrier and its alteration in immune mediated neuropathies. J Neurol Neurosurg Psychiatry. 84: 208-212.
49. Kurt Incesu T, Secil Y, Tokucoglu F, Gurgor N, Özdemirkiran T, et al. (2013). Diagnostic value of lumbar root stimulation at the early stage of Guillain-Barré syndrome. Clin Neurophysiol. 124: 197-203.
50. Sevy A, Grapperon AM, Salort Campana E, Delmont E, Attarian S.(2018). Detection of proximal conduction blocks using a triple stimulation technique improves the early diagnosis of Guillain-Barré syndrome. Clin Neurophysiol 129: 127-132.